



UNIVERSITY OF LEEDS

This is a repository copy of *Effects of friction conditions on the formation of dead metal zone in orthogonal cutting – a finite element study*.

White Rose Research Online URL for this paper:
<http://eprints.whiterose.ac.uk/126428/>

Version: Accepted Version

Article:

Wan, L, Haddag, B, Wang, D et al. (2 more authors) (2018) Effects of friction conditions on the formation of dead metal zone in orthogonal cutting – a finite element study. *Machining Science and Technology*, 22 (6). pp. 934-952. ISSN 1091-0344

<https://doi.org/10.1080/10910344.2018.1429469>

(c) 2018 Taylor & Francis Group, LLC. This is an Accepted Manuscript of an article published by Taylor & Francis in *Machining Science and Technology* on 9/03/2018, available online: <https://doi.org/10.1080/10910344.2018.1429469>

Reuse

Items deposited in White Rose Research Online are protected by copyright, with all rights reserved unless indicated otherwise. They may be downloaded and/or printed for private study, or other acts as permitted by national copyright laws. The publisher or other rights holders may allow further reproduction and re-use of the full text version. This is indicated by the licence information on the White Rose Research Online record for the item.

Takedown

If you consider content in White Rose Research Online to be in breach of UK law, please notify us by emailing eprints@whiterose.ac.uk including the URL of the record and the reason for the withdrawal request.



eprints@whiterose.ac.uk
<https://eprints.whiterose.ac.uk/>

Effects of Friction Conditions on the Formation of Dead Metal Zone in Orthogonal Cutting – a Finite Element Study

Lei Wan^{1, 2}, Badis Haddag³, Dazhong Wang², Yong Sheng¹, Dongmin Yang^{1,*}

¹School of Civil Engineering, University of Leeds, LS2 9JT, UK

²School of Mechanical Engineering, Shanghai University of Engineering Science, 333 Longteng Road, 201620, Shanghai, China

³University of Lorraine, Laboratoire d'Energétique et de Mécanique Théorique et Appliquée, LEMTA CNRS-UMR 7563, Mines Nancy, Mines Albi, GIP-InSIC, 27 rue d'Hellieule, 88100 Saint-Dié-des-Vosges, France

Abstract: A numerical study of the effects of friction conditions on the formation of dead metal zone (DMZ) is presented. The friction conditions are classified as three different cases in the form of coefficient: (1) constant coefficient of friction, (2) ‘smooth’ and ‘sharp’ change of the friction coefficient and (3) time-dependent friction coefficient. These friction cases are numerically investigated using the finite element (FE) code ABAQUS/Explicit. A FE model based on the arbitrary-Lagrangian-Eulerian approach is developed to simulate the cutting process and investigate the influences of the friction conditions. The simulated results, for a wide range of friction conditions, are obtained, analyzed and compared with previously published experimental/numerical data. It has been found that the friction coefficient has a direct effect on the amount and shape of DMZ, the sharp change of coefficient has a larger effect on the DMZ formation than the smooth one, and the formation of DMZ is more determined by the value of the friction coefficient than its duration.

Keywords: Metals machining; Dead Metal Zone; Tribological behaviour; Friction effect;

* Corresponding author. Email: d.yang@leeds.ac.uk

Finite Element Analysis

1. Introduction

The tool edge geometry is of crucial importance during the machining process. For a given cutting condition, the tool edge geometry has significant influences on the cutting forces, tool wear or tool life, chip formation and machined surface integrity (Fulemova and Janda, 2014). Associated with the tool edge geometry there is also an interesting phenomenon called the formation of “dead metal zone” (DMZ) in the vicinity of tool edge during the continuous ductile-metal cutting process. The DMZ is formed under the tool edge and acts as a new cutting edge to prevent the tool edge from wear and affect the roughness of the machined surface (Jacobson and Wallén, 1988). After cutting, the DMZ deposits on the rake face of the tool in a form of built-up edge. Most of the literatures are focused on the built-up edge, such as (Atlati et al., 2015; Childs, 2013; Iwata and Ueda, 1980; Kümmel et al., 2015; Kummel et al., 2014; Oliaei and Karpas, 2016; Uhlmann et al., 2015), whilst only few of them investigated the DMZ. In contrast, the DMZ phenomenon has been studied in extrusion machining for a long time, such as (Alexandrov et al., 2001; Eivani and Taheri, 2008; Lee et al., 2012; Misiolek and Kelly, 1993; Misiolek and Kialka, 1996; Qamar, 2010; Segal, 2003a).

The DMZ phenomenon was firstly investigated in 1988 by Jacobson and Wallén et al. (Jacobson and Wallén, 1988; Jacobson et al., 1988; Wallén et al., 1988). They proposed a classification for the DMZ based on the localization of two separating cracks that result in the chip and machined surface respectively. Meanwhile, they concluded that the form and size of DMZ is unstable as it could crack partially or sometimes completely under thermo-mechanical effects to largely influence the cutting process and the integrity of the machined surface. Hirao

et al. (Hirao et al., 1982) and Zhang et al. (Zhang et al., 1991) concluded from the experimental findings that the chip thickness is not affected by the chamfer angle because of the DMZ, which can effectively fill in the missing edge under the chamfer and act as the cutting edge. Movahhedy et al. (Movahhedy et al., 2002) conducted several thermo-mechanical adaptive Lagrangian-Eulerian (ALE) simulations of chip formation in cutting processes with different types of chamfer tools. They observed the phenomenon of DMZ formation in the FE simulations and concluded that the chamfer angle has no influence on the chip formation significantly due to the existence of DMZ. Later, Karpal and Özel (Karpal and Özel, 2007) proposed a novel analytical model of the DMZ in high-speed machining with chamfered tools. They found that the DMZ exists under the chamfer edge or in the vicinity of the worn part in different cutting conditions, and concluded the DMZ mostly depends on the geometrical profile of the tool edge instead of the cutting variables. Wan and Wang (Wan and Wang, 2015) investigated the effects of tool edge geometry and friction coefficient on the formation of DMZ by FE simulations and experimental validations. They found the tool edge and friction coefficient are both responsible for the DMZ formation. Afsharhaneai et al. (Afsharhaneai et al.) carried out experiments and simulations on AISI 1045 to investigate the effects of the formation of dead metal cap on the machining process outputs (i.e. cutting forces, thrust forces and chip thickness), stress distributions and temperature fields in orthogonal micromachining. They found that the process outputs are highly dependent on the formation and geometry of dead metal cap and the accuracy of the FE predictions can be significantly improved by introducing the dead metal cap.

During the metal cutting process one of the most important issues is the tribological

behaviour at the tool-chip interface and its effects on the machining process variables. Theoretically, Zorev (Zorev, 1963) proposed a friction model, in which the contact zone is divided into two regions, as shown in Fig. 1. The first zone is a sticking zone where the normal stress decreases slowly from the tip of tool to the separation point of the chip and the tool. The second one is a sliding zone where the frictional shear stress remains the same until the end of the sticking zone and then decreases from the beginning of the sliding zone towards the same position where the normal stress vanishes. The same trend was validated experimentally by Usui and Takeyama (Usui and Takeyama, 1960), where both the frictional and normal stresses were measured, and by Yamaguchi and Yamada (Yamaguchi and Yamada, 1972) with a unique dynamometer. Wu et al. (Wu et al., 1996) modified Zorev's model by assuming that equal lengths of the sticking and sliding zones, while the frictional shear stress has certain relationship with the stresses in the sticking zone and linearly decreases down to zero in the sliding zone.

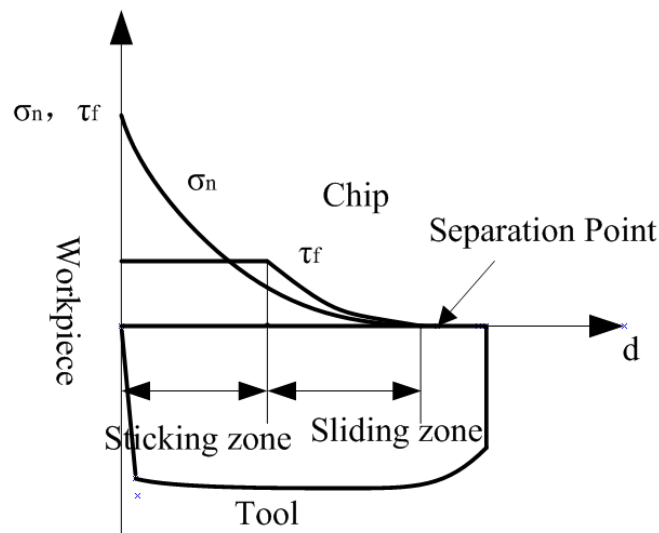


Fig. 1. Distributions of normal and frictional stresses on the tool rake face in Zorev's friction model (Zorev, 1963).

On the other hand, FE method has been used to analyse the mechanism of DZM. Arrazola and Özel (Arrazola and Özel, 2010) investigated the tribological behaviour during the cutting process of homogeneous isotropic metal using an ALE approach with Eulerian and Lagrangian chip boundaries. They found that in the ALE model with Eulerian boundary, the obtained results are the same for both Coulomb friction model and sticking-sliding friction model when the maximum shear stress is set to be higher than 500 MPa. Özel (Özel, 2006) studied the effects of various friction models by introducing friction coefficient based models in their FE simulations. Filice et al. (Filice et al., 2007) compared three friction models, i.e. Coulomb friction law, constant shear model and Zorev's model (Zorev, 1963), and found that the main mechanical outputs (i.e. cutting forces, contact length, chip thickness and so on) are not sensitive to the friction model, whilst the temperature field is sensitive since the friction determines the heat generated at the rake face. Haddag et al. (Haddag et al., 2014a; Haddag et al., 2014b) found that tribological behaviour at the tool-chip interface is largely influenced by tool edge geometry, which results in the deposit of the built-up edge (BUE) on the grooved rake face, even when the multilayer coating was used. Recently, Atlati et al. (Atlati et al., 2015) investigated the effects of friction coefficient and tribology behaviour on the formation of BUE when cutting ductile metals. They considered the effects of an abrupt change and a gradual evolution of the friction coefficient on the BUE formation as well as the sticking zone length and the plastic strain in the second deformation zone. Similar friction problems also exist in extrusion processes as well, for example, Segal (Segal, 2003b) studied the effects of different friction conditions on the non-uniform, variable deformation modes and complicated loading history. And they found that the friction at material-wall interface and DMZ can be eliminated

by the movable channel walls which change the extrusion processing mechanisms. These approaches can be applied to investigate the DMZ formation under the effects of different friction conditions. In addition, there are several differences and similarities between the BUE and the DMZ, as shown in Fig. 2. The BUE mainly exists on the rake face of tool with any geometry while DMZ mainly occurs under the tool edge of a chamfer tool. For example, it is easy to find the BUE phenomenon with a round tool under a cutting condition while it is hard to recognize the DMZ as the round edge helps to enhance the material flow. Moreover, the DMZ only occurs during the cutting process and would remain on the rake face of tool in the form of BUE after cutting.

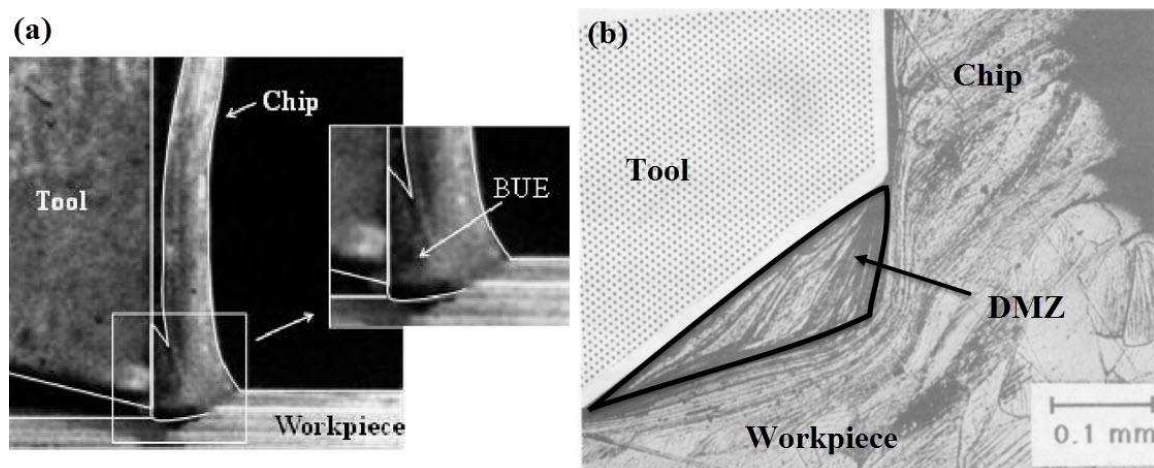


Fig. 2 Comparisons between (a) BUE (Atlari et al., 2015) and (b) DMZ (Jacobson and Wallén, 1988).

Despite many efforts have been made to understand the friction mechanism in different machining processes or during the BUE formation, the tribological behaviour is still difficult to evaluate experimentally due to the intensive thermo-mechanical loading in a very small region, where the coefficient of friction cannot be measured directly. For this reason, this paper aims to numerically investigate the effects of different friction conditions on the formation of

DMZ during the cutting process, which could help to better understand the mechanism of the DMZ formation and potentially optimize the geometrical design of extrusion. For this purpose, three different friction conditions defined by friction coefficient are considered, including constant friction coefficient, gradual and abrupt change of friction coefficient and time-dependent friction coefficient. A 2D ALE finite element model of cutting process is established to predict the DMZ formation. The simulation results are discussed to interpret the effects of the different friction conditions on the thermo-mechanical fields around the DMZ.

2. Finite Element Modelling of DMZ

A cutting process usually involves complex phenomena, which often necessitate numerical approaches to reproduce them and then to analyze the effect of pertinent parameters. To analyze the DMZ formation in machining, a FE model is developed with a focus on the effect of friction conditions. The model is described hereafter and the friction conditions are defined afterward.

2.1. Finite Element Modelling of Orthogonal Cutting

A 2D plane strain ALE FE model for orthogonal cutting is illustrated in Fig. 3. A similar model has been validated for simulating the deformation of continuous chips under a steady state cutting in our previous work (Wan and Wang, 2015). Compared to the model in (Wan and Wang, 2015), this model in Fig.3 has a larger uncut chip thickness and a lower cutting speed in order to acquire DMZ more easily. The FE model consists of a deformable workpiece (20 mm of length, 10 mm of height, and 1 mm of uncut chip thickness), and a tool (rake angle of 10° , clearance angle of 7° and chamfer with 0.25 mm). A chamfer tool is utilized in this model as the DMZ formation with the chamfer tool is much easier to be obtained, compared to sharp,

double chamfer and blunt tools (Movahhedy et al., 2002; Wan and Wang, 2015). Considering the stability of the formation of DMZ, the cutting speed is set to 1 m/s. The workpiece is meshed with combined strain thermo-mechanical four-node quadrilateral elements (CPE4RT) and the tool is meshed with 3-nodes plane strain thermo-mechanical coupled triangle elements (CPE3T). A typical refined mesh is applied in the primary deformation zone (PDZ), chip surfaces and in the tool as shown in Fig. 3. An automatic remeshing method is applied to avoid excessive distortion of elements in the primary and secondary zones during the simulation. Fig. 3 also shows the basic geometry with boundary conditions. At the boundaries of the workpiece which are defined by Eulerian method, material enters from the left with a specified cutting speed and exists at the right boundary as well as the chip's top surface, while the tool is fixed. Elements at the left and right hands of the workpiece are constrained in the cutting direction (X direction) to control the Eulerian boundaries as same as the chip's top in the feed direction (Y direction). At the surface of the workpiece there is no constraint and the mesh in that region moves with the material in a Lagrangian way. The initial shape of the chip can evolve freely to satisfy the cutting condition (Haglund et al., 2008).

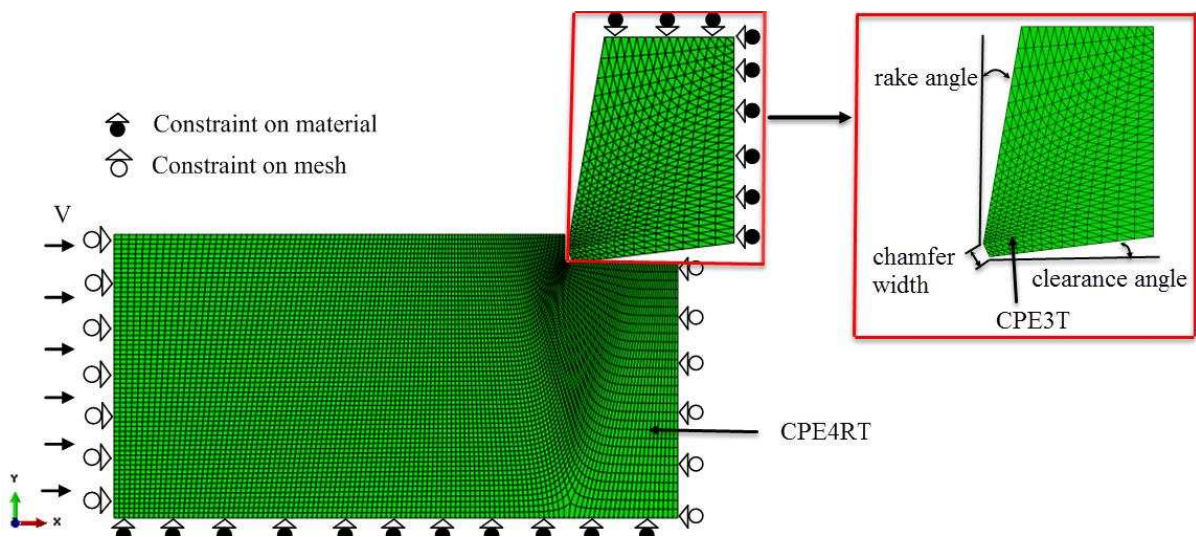


Fig. 3. 2D-ALE FE model (plane strain condition) for orthogonal cutting with a chamfered tool.

2.2. Material Model

The thermo-mechanical behaviour of the work material is governed by the classical Johnson-Cook flow stress law (Johnson and Cook, 1983), given as follow:

$$\bar{\sigma} = \left[A + B\bar{\varepsilon}^n \right] \left[1 + C \ln \left(\frac{\dot{\bar{\varepsilon}}}{\dot{\bar{\varepsilon}}_0} \right) \right] \left[1 - \left(\frac{T - T_r}{T_m - T_r} \right)^m \right] \quad (1)$$

where $\bar{\sigma}$ is the equivalent flow stress, $\bar{\varepsilon}$ the equivalent plastic strain, $\dot{\bar{\varepsilon}}$ the equivalent plastic strain rate, $\dot{\bar{\varepsilon}}_0$ the reference strain rate, T the temperature, T_r the reference temperature, T_m the melting temperature, n the strain hardening coefficient, C the strain-rate sensitivity coefficient, and m the thermal softening coefficient. Johnson-Cook parameters of the machined metal AISI 4340 are listed in Table 1 and material properties for the workpiece and tool are listed in Table 2 (Arrazola and Özel, 2010).

Table 1. Johnson-Cook viscoplastic parameters of AISI 4340 (Arrazola and Özel, 2010).

A (MPa)	B (MPa)	n	C	m	$\dot{\bar{\varepsilon}}_0$
792	510	0.26	0.014	1.03	1

Table 2. Physical properties of workpiece and tool material (Arrazola and Özel, 2010).

Properties	Workpiece (AISI 4340)	Tool (Carbide)
Density (kg.m ⁻³)	7850	15000
Young's modulus (GPa)	208	800
Poisson ratio	0.22	0.2
Conductivity(W.m ⁻¹ .°C ⁻¹)	44.5	46
Specific heat (J.kg ⁻¹ .°C ⁻¹)	477	203
Thermal expansion coefficient (°C ⁻¹)	1.23×10 ⁻⁶	4.7×10 ⁻⁶
Reference temperature (°C)	25	25
Melting temperature (°C)	1460	-

2.3.Friction Model

The friction model has a significant impact on simulated thermo-mechanical quantities in metal machining (e.g. stress, strain and temperature and flow velocity distributions). In this study we adopt the Zorev's model (Zorev, 1963) as already shown in Fig. 1, in which the maximum normal stress occurs at the edge of tool to allow chip separation from the workpiece. The normal stress decreases gradually from its maximum down to zero when the chip leaves the tool under the deformation and friction. The friction stress stays the same at the sticking region on the tool rake face, and then gradually decreases to zero in the sliding zone.

Considering the sticking and sliding behaviour at the tool-chip interface, the friction during the cutting process can be governed by the Coulomb-Orowan law, expressed as follow:

$$\tau_f = \min\left(\mu \cdot \sigma_n, \tau_{lim} = m \cdot \bar{\sigma} / \sqrt{3}\right) \quad (2)$$

where τ_f is the friction (sliding) stress, σ_n the normal friction stress, $\bar{\sigma}$ the flow stress of the work material, μ the COF, τ_{lim} the friction (sliding) stress limit, and m the friction limit factor. When $\tau_f = \mu \cdot \sigma_n$ there is a sliding contact, else (i.e. $\tau_f = \tau_{lim}$) there is a sticking

contact.

3. Friction Conditions for the Analysis of DMZ

Atlati et al. (Atlati et al., 2015) proposed a time-independent friction coefficient to investigate the effects of an abrupt or gradual evolution of coefficient on the cutting process. Based on this approach, three different friction conditions are considered in this study: (i) constant friction coefficient, (ii) three friction coefficients with smooth or sharp changes and (iii) change of friction coefficient with time (time-dependent friction). Table 3 shows the schematic diagrams for the later two friction conditions.

Table 3. Illustration of different friction conditions.

Friction condition	Schematic diagram
(a) Friction coefficient with smooth or sharp changes	
(b) Change of friction coefficient with time	

3.1. Constant friction coefficient

In the first friction condition, a constant friction coefficient is implemented into the Coulomb friction model to investigate the tribological behaviour at the tool–chip interface. Sensitivity study of ten different friction coefficients, ranging from 0.1 to 1, is conducted to evaluate their

effects on the DMZ formation as well as the cutting process.

3.2. Friction coefficient with smooth or sharp change

In the second friction condition, the friction coefficient in the Coulomb friction model is not considered as constant but increases with the computation steps during each FE simulation of the cutting process. The initial value of the friction coefficient is set to 0.2 and three different increments are considered, i.e. 0.1, 0.2 and 0.3. The first case with an increment of 0.1 represents a ‘smooth change’ of the friction, whilst the rest two cases represent relatively ‘sharp change’ of friction, which can be found in the Table 3(a).

3.3. Change of friction coefficient with time

In the third friction condition, the friction coefficient varies with time to investigate the effects of the duration of friction on the DMZ formation, which is shown in Table 3(b). The friction coefficient increases from 0.2 to a certain value and remains constant for different periods of time before dropping down to the original value. Here in this study, in step one, the coefficient is 0.2 for 0.002s, while in step two it increases to 0.4 and lasts for 0.001s, 0.002s and 0.003s, respectively, and eventually it descends to 0.2 and lasts for 0.003s, 0.002s and 0.001s, respectively. The total time for each FE simulation is 0.006s. These changes of friction coefficient will directly influence the DMZ formation, as indicated by the shape of DMZ and the evolution of cutting forces during the cutting process hereafter.

4. Results and discussion

4.1. Formation of the DMZ

The existence of the DMZ in the vicinity of tool edge is a very interesting phenomenon when studying the metal cutting process, because it just occurs during the cutting process, disappears when the cutting process is completed and finally stays on the rake face of tool near its tip,

resulting in the BUE. The formation of DMZ is investigated with the distributions of velocity field and some other quantities (e.g. stress and strain). Fig. 4 shows the distribution of flow velocity, stress and temperature fields in the 2D FE simulations with a cutting speed of 1 m/s. Fig. 4(a) shows that the material flow is blocked due to the existence of the tool chamfer and tends to fill in the spare space to form the DMZ, acting as a local cutting edge to protect the tool edge from wear. The highest Von Mises stress is observed in the PDZ, spanning from the end of free surface on workpiece to the edge of the DMZ as shown in Fig. 4(b).] The DMZ at the chamfered tool tip changes the position of the PDZ compared to those without DMZ formation. Fig. 4(c) shows that the regions with maximum temperature locates at the second and third deformation zones as well as around the chamfer edge of the tool, as a result of the combined effects of friction heat and plastic deformation energy which is converted to heat in these regions.

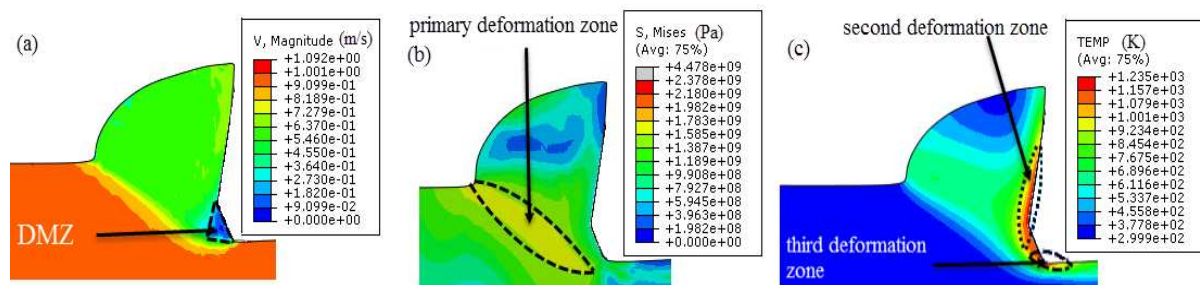


Fig. 4. Distribution of (a) flow velocity field, (b) Von Mises stress and (c) temperature during chip formation ($V_c = 1$ m/s and $d_{uncut} = 1$ mm, COF = 0.5).

4. 2. Effect of constant COF on DMZ

Considering the formation of DMZ occurs near the tool tip where there are some physical and chemical phenomena due to the strong contact, so the influences of the friction conditions on its formation need to be investigated. In this study, an area that contains a velocity of material less than 10% of the working velocity is assumed to be a DMZ. Fig. 5 shows the effect of constant COF on the DMZ formation under cutting speed of 1 m/s. It is shown that the increase

of COF can result in an increase of the size of DMZ. This is due to the severe friction at the interface between tool and chip, which makes material in the chip flow much harder and an increase of material accumulation around the edge. The difference between the flow velocity fields in the DMZ, as shown in Fig. 5, is not significant which suggests a small change of the COF does not affect the DMZ formation. It is obvious that the DMZ formation is easier to occur under a higher friction coefficient.

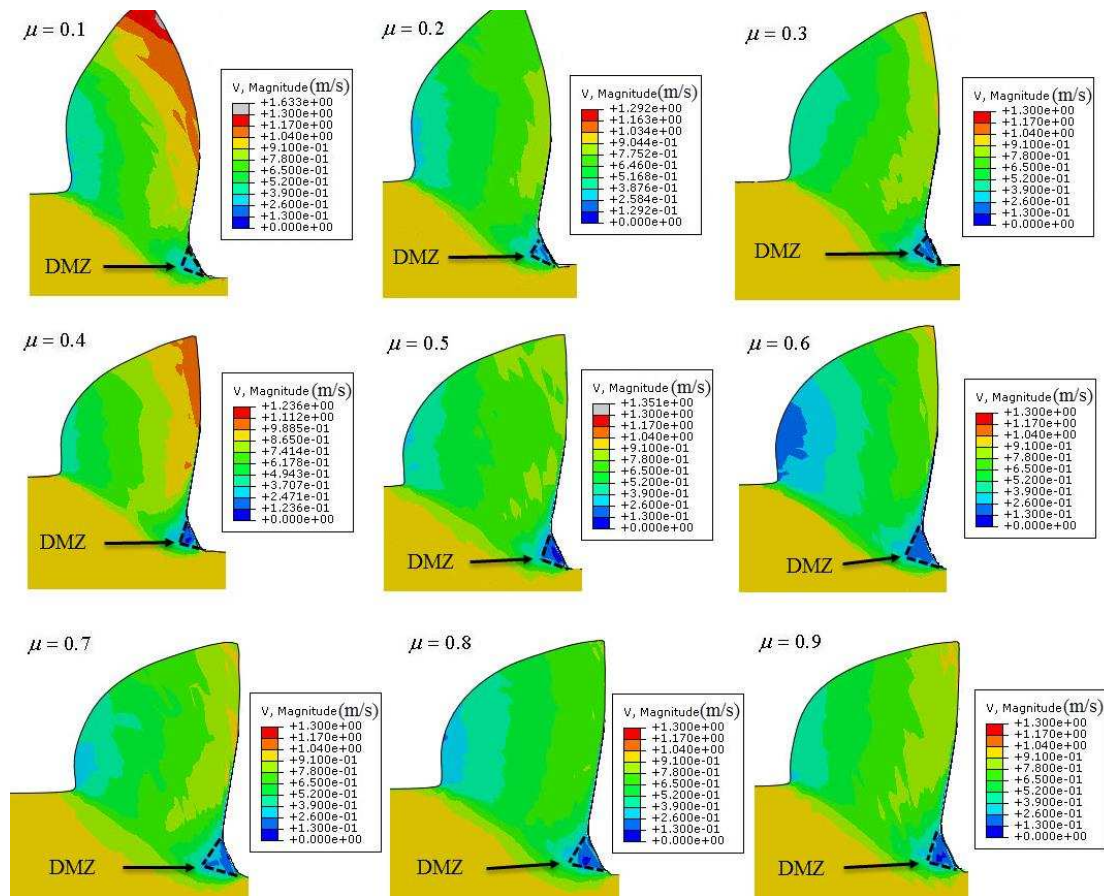


Fig. 5. Flow velocity field for constant COF (0.1 to 0.9).

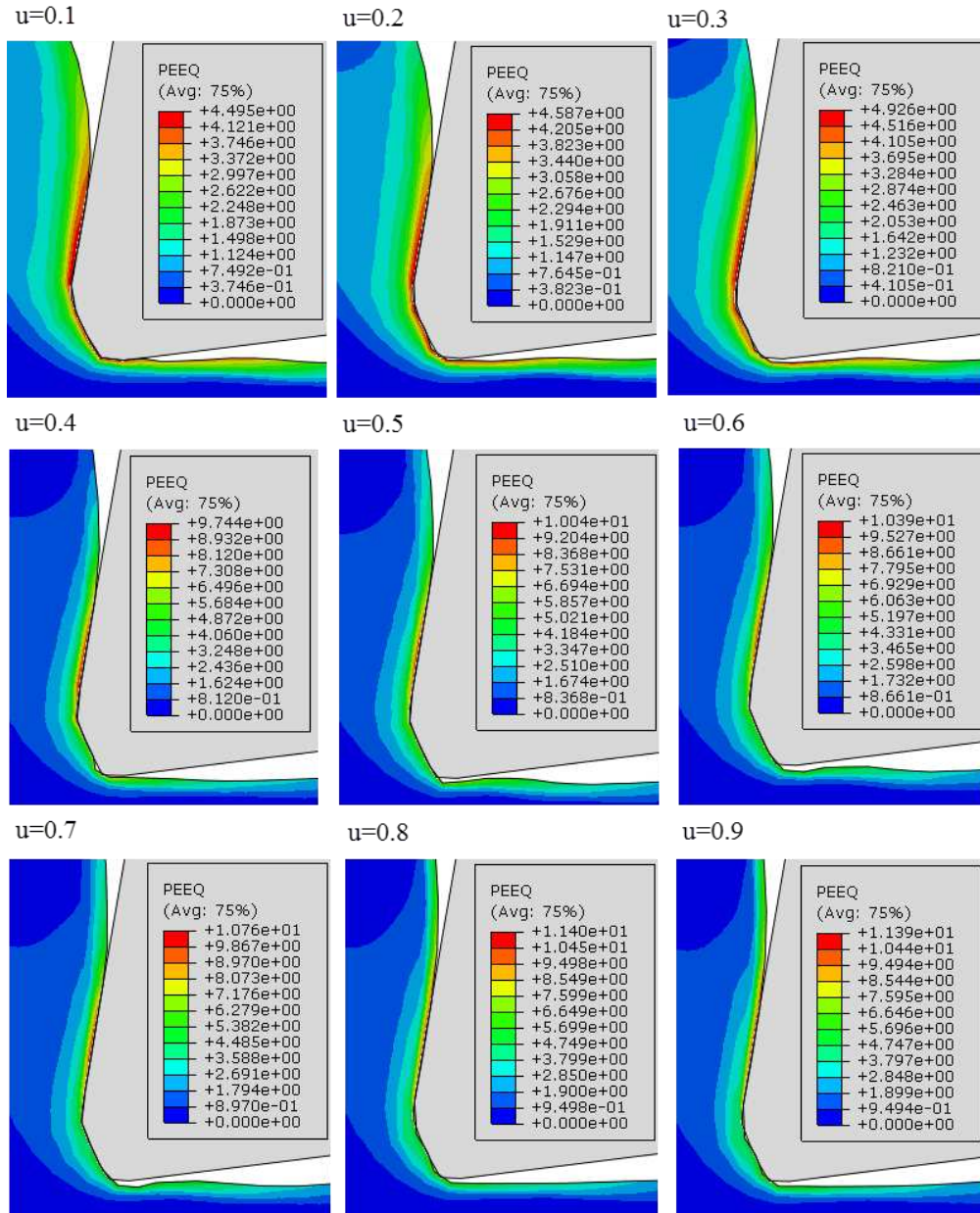


Fig. 6. Plastic strain field for constant COF (0.1 to 0.9).

In addition, a similar effect of the COF on the equivalent plastic strain field for different frictions (COF from 0.1 to 0.9) can be observed in Fig. 6. It can be found that the maximum strain increases from 4.4 to 11.4 when COF passes from 0.1 to 0.9, suggesting the material endures a severe deformation at interface between tool and chip which slows down material flow at the interface and in the vicinity of the edge where the DMZ occurs.

Meanwhile, the increase of plastic strain due to the deformation and friction can result in the

increase of maximum temperature in all three deformation zones. The same trend can be found in Fig. 7, which presents the temperature fields with different COFs. The maximum temperature in the secondary zone and around the tool tip increases largely from 1260 K to 1472 K when the COF increases from 0.1 to 0.9, which promotes the adhesion of the material under the tool chamfer and consequently leads to the deposit of BUE (formation of built-up layer).

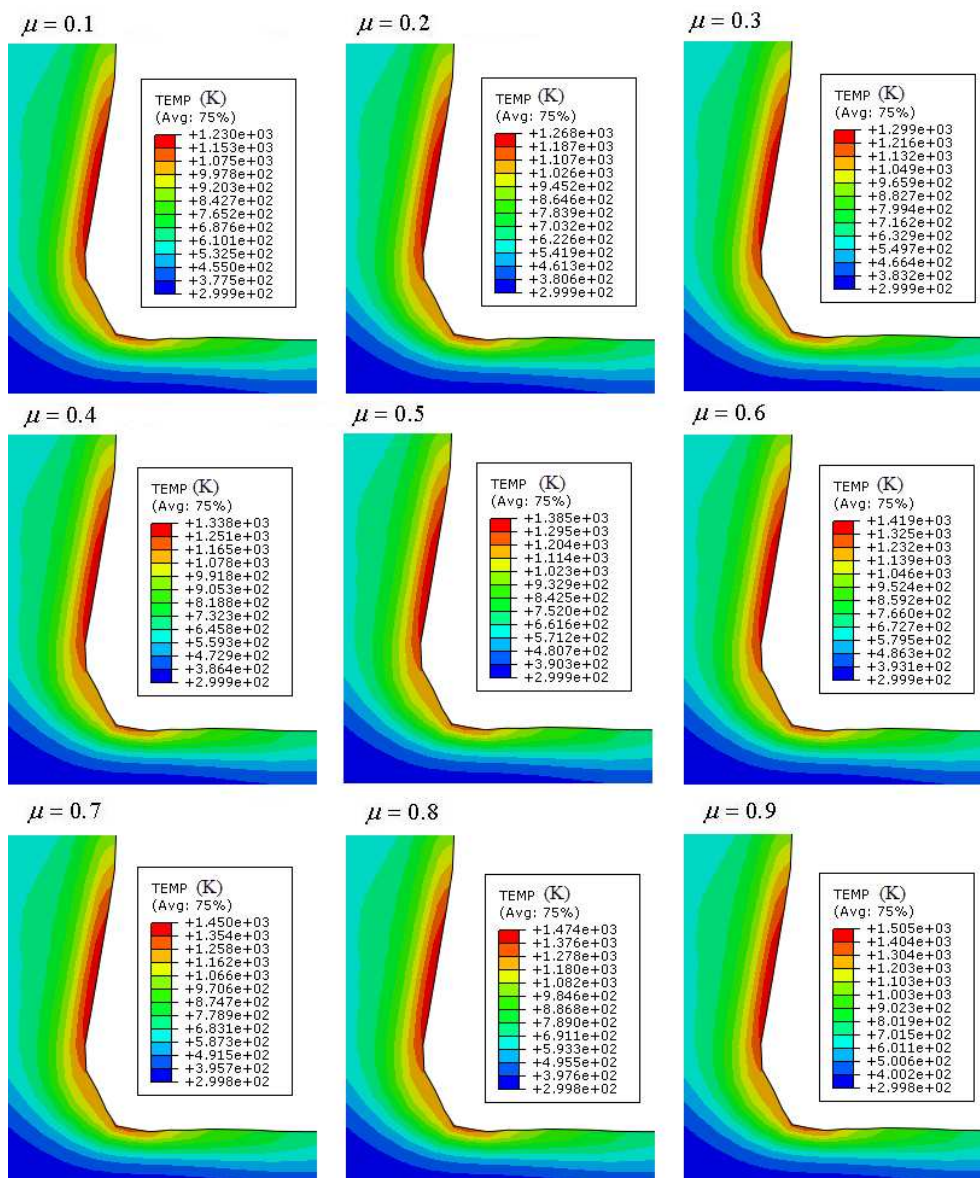


Fig. 7. Temperature field for constant COF (0.1 to 0.9).

The effect of friction at the tool-chip interface on the magnitude of cutting and thrust

forces is also investigated, as reported in Fig. 8. The forces fluctuate slightly during the simulations probably because of the adaptive meshing used in the ALE FE model. Meanwhile, the increase of the thrust force (130%) is two times larger than the cutting force (50%) as the COF increases from 0.1 to 1. It can be concluded that the thrust force, compared to the cutting force, is more dependent on the COF, which is in accordance with the size of DMZ. Increase of the DMZ makes the material flow more difficult to form the chip during the cutting process and hence lifts up the thrust force.

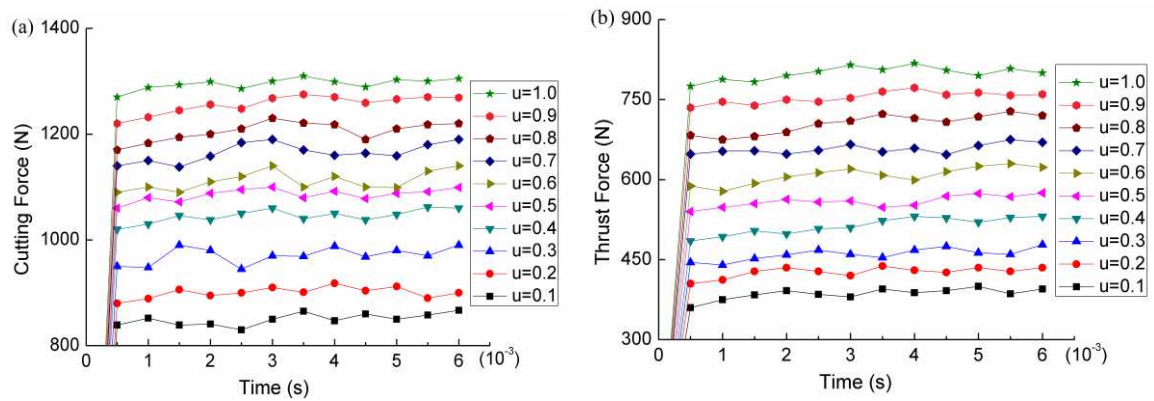


Fig. 8. Effect of constant COF on (a) cutting force and (b) thrust force.

4.3. Effect of smooth and sharp changes of COF on DMZ

The second friction condition involves smooth and sharp changes of COF during the cutting process. Details of this condition are reported in Table 3. The increment of COF is taken from 0.1 to 0.3, which can be regarded as smooth or sharp change, such as (0.2, 0.3, 0.4) for smooth change, and (0.2, 0.4, 0.6) and (0.2, 0.5, 0.8) for sharp change.

Table 4. Flow velocity field for smooth and sharp changes of the COF.

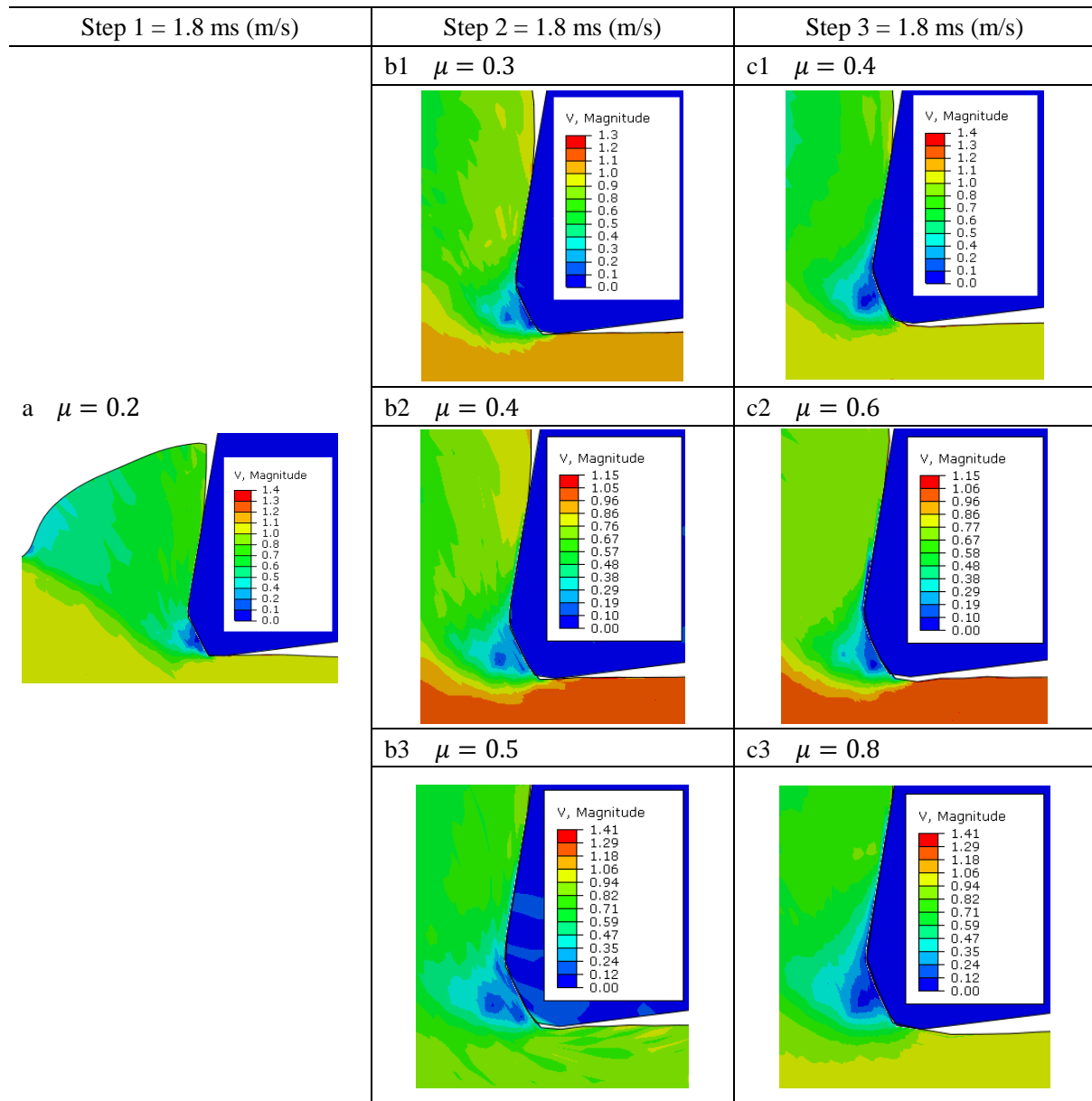
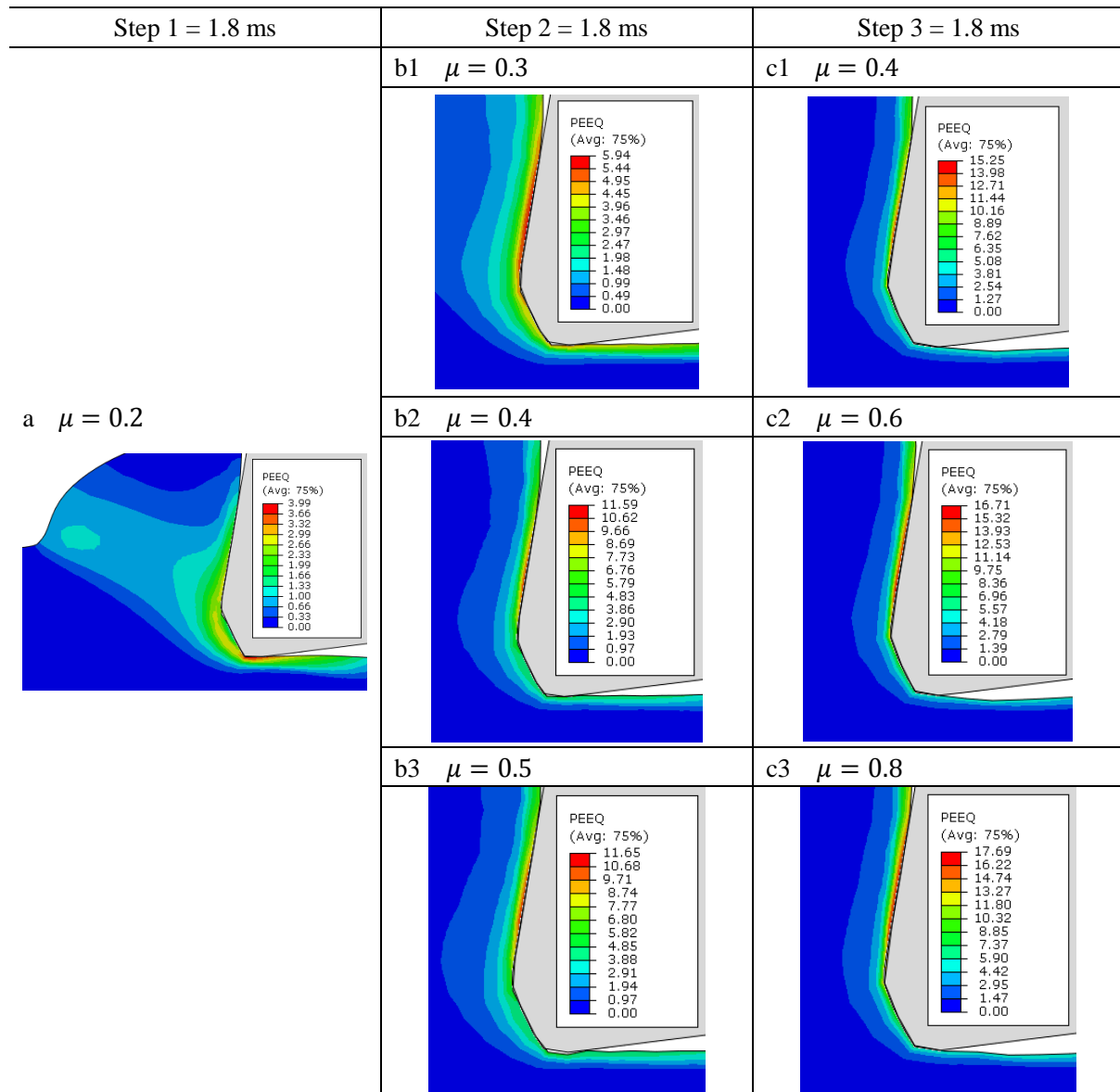


Table 4 shows the effect of smooth and sharp changes of the COF on the flow velocity distribution around the tool tip. In these simulations, three steps are defined. Every step lasts 2 ms and the screenshot images are taken at 1.8 ms in each case. From the first set of simulations (Table 4(a)-(b1)-(c1)), the size of the DMZ increases gradually as the COF increases from 0.2 to 0.4 with an increment of 0.1. At the end, the DMZ formed under the tool chamfer, resulting in the deposition on the rake face in the form of the BUE. But from the second set of the

simulations (Table 4(a)-(b2)-(c2)), when the COF varied from 0.2 to 0.6 with an increment of 0.2, the shape and size of the DMZ varies largely, increasing to the largest when the COF is 0.4 and then decreasing back to a small one. This indicates that the DMZ accumulates to a certain degree and then cracks and vanishes along with the material flow. Indeed, the DMZ size in Table 4(c2) with the coefficient of 0.6 is almost same as the one in Table 4(a) with the coefficient of 0.2, suggesting that the formation of the DMZ is unstable and sometimes cracks during the process. For the third case that represents a severe friction change, the DMZ formation increases significantly, as reported in Table 4(a)-(b3)-(c3). The shape of the DMZ in Table 4(c3) is very similar with the one in Table 4(c1), suggesting more material deposit on the rake face at the end of cutting, leading to the BUE. Considering the increment of the COF, it can be concluded that a large gap of friction coefficient between two adjacent steps generally results in a large accumulation of the DMZ. As the simulation advances, the DMZ varies in both form and size, illustrating its instability during the cutting process, which can also be found in Jacobson and Wallén (Jacobson and Wallén, 1988).

Table 5. Plastic strain field for smooth and sharp changes of the COF.



Friction change also has an effect on the plastic strain distribution in the vicinity of the tool edge, as reported in Table 5. The first set of simulations, with the increment of 0.1 for the COF, suggests that the maximum strain increases as the friction increases, however there is a large gap of strain between step 2 and step 3 (COF from 0.3 to 0.4). For the second and third cases, the increase of maximum strain is almost 50% and 60% when the COF increments are 0.2 and 0.3, respectively. Comparisons of the three sets of simulations show that the larger plastic strain results from the larger gap between the two adjacent steps, while when the COF reaches relatively high, the gap between two steps has little effect on the final value of strain.

4.4. Time-dependent COF

The third friction condition regards a time-dependent friction. Indeed, the friction is so complicated that it cannot be considered as constant and would change without an obvious law. This is proved by the fact that adhesion of material occurs progressively on the tool tip and/or rake face, and then adhered material detaches progressively. So the progressive adhesion and detaching of material can be associated with an increase and decrease of friction accordingly. A few scenarios have been proposed by Atlati et al. (Atlati et al., 2015), as below: (1) COF increases to a certain value and then decreases to the former one, such as (0.2, 0.3, 0.2), (0.2, 0.4, 0.2) or (0.2, 0.5, 0.2) in three different steps, respectively; (2) COF decreases to a certain value and then increases back to the former one, such as (0.4, 0.2, 0.4); and (3) COF increases to a certain value, remains constant for different time, and then returns to the former one. For example, COF is 0.2 for 0.002s in step one and increases to 0.4 for 0.001s, 0.002s and 0.003s in step two, respectively, at last it drops back to 0.2 for 0.002s in step three. These changes of coefficient would directly affect the DMZ formation. Therefore, a new method combining (1) and (3) is applied in this study to study the effects of duration of the friction contact on the formation of the DMZ, and the details can be found in Chapter 3.3.

Table 6. Flow velocity field for time-dependent COF.

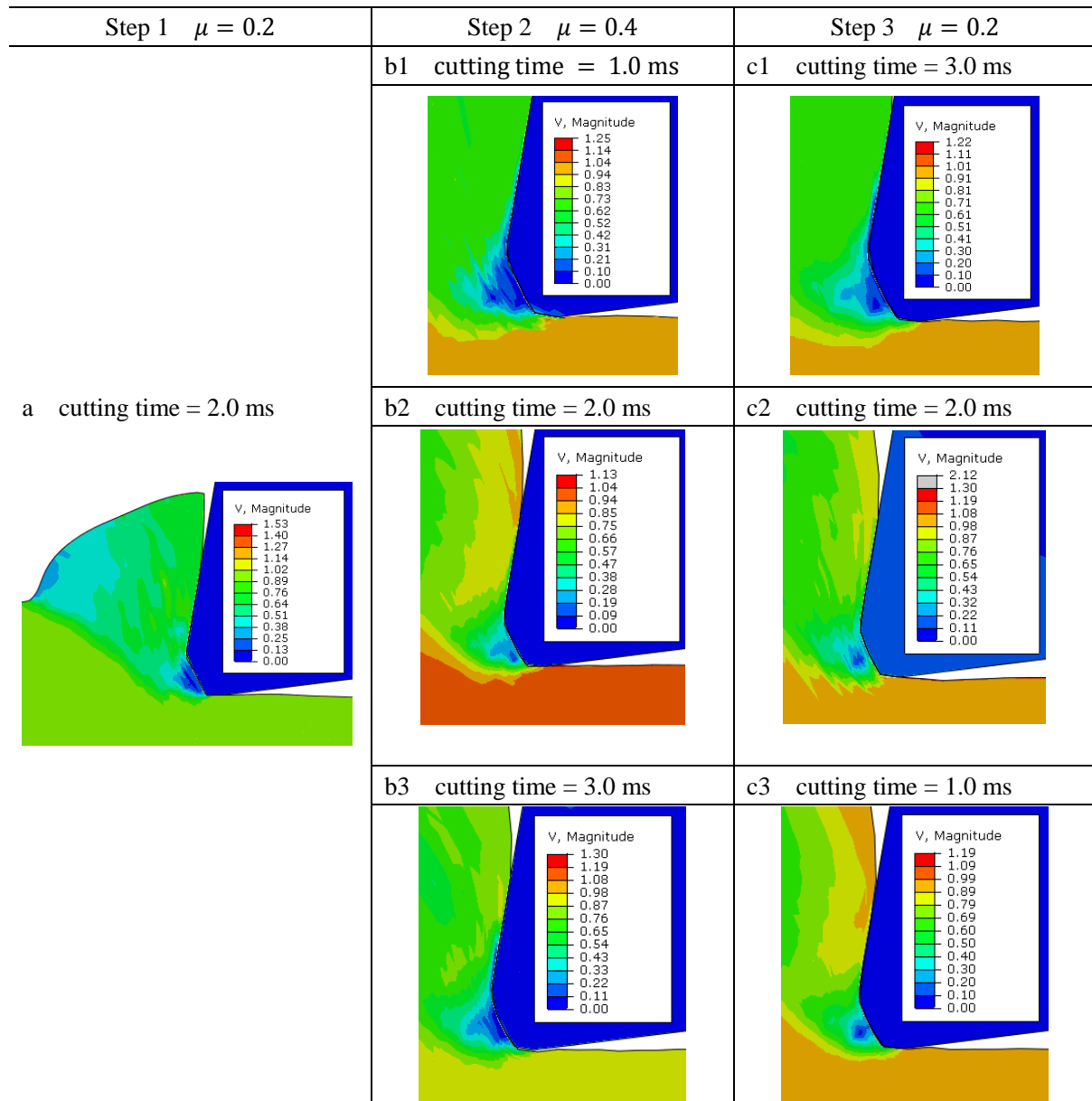
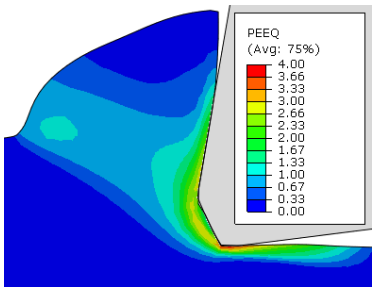
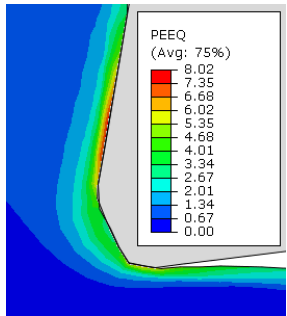
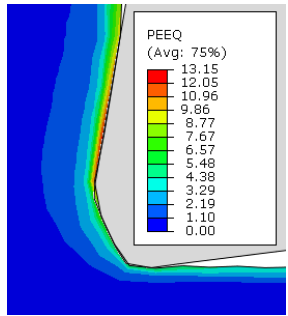
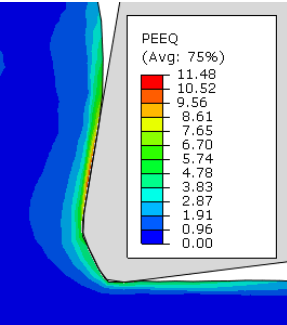
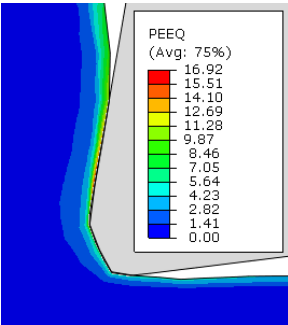
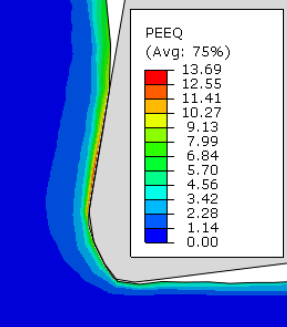
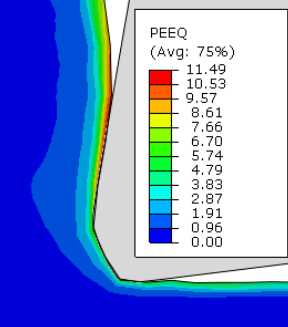


Table 6 shows the effect of changing friction at different steps on the distribution of the velocity field around the tool tip. It can be found that for all cases the cutting time in step 2 (friction increase) and step 3 (friction decrease) has a direct effect on the DMZ size. This suggests that in a real cutting process the DMZ may be unstable and its shape and size may change during the cutting process.

This friction condition also affects the plastic strain distribution at the cutting zone. It can be seen in Table 7 that the distribution and maximum value of plastic strain clearly depends on the cutting time in steps 2 and 3. Comparing the second case with first case, it can be found that a longer duration in the step 2 results in a larger equivalent strain under the same friction condition. From the third one, it can be concluded that the friction could decrease when the time duration of the friction is shorter, compared to the former two cases.

Table 7. Plastic strain field for time-dependent COF.

Step 1 $\mu = 0.2$	Step 2 $\mu = 0.4$	Step 3 a $\mu = 0.2$
a cutting time = 2.0 ms 	b1 cutting time = 1.0 ms 	c1 cutting time = 3.0 ms 
	b2 cutting time = 2.0 ms 	c2 cutting time = 2.0 ms 
	b3 cutting time = 3.0 ms 	c3 cutting time = 1.0 ms 

5. Conclusions

Tribological behaviour at the interface of tool–chip during the orthogonal cutting process of AISI 4340 steel with a chamfer tool is investigated by FE modelling. The study is particularly focused on the influences of friction conditions on the formation of the DMZ. Concluding remarks are drawn as follow:

(1) The DMZ is blocked under the chamfer of tool and it varies in form and size during cutting.

The material around the tool tip experiences a severe deformation which can be verified by predicted strain, stress and temperature distributions. The flow velocity field can be used as an indicator of the existence and amount of the DMZ.

(2) The friction condition has a direct effect on the shape and size of the DMZ. Increasing the friction coefficient increases the DMZ size. A sharp change of coefficient of friction has larger influence on the DMZ formation than a smooth change of friction coefficient.

(3) The change of friction coefficient with time has also an effect on the DMZ formation. The time duration of cutting has an effect on the DMZ size when friction increases and then decreases, but the value of friction coefficient has more influences than the duration on the DMZ formation.

(4) Finally, this parametric study provides a reference for future experimental validations of the chosen variables. The friction condition in this study is still simplified and the expression of friction conditions (and the friction model) should be improved by incorporating the time duration of cutting. In addition, more experimental data are also required to validate the parameters chosen in this study.

References

- Afsharhanaei, A.; Rebaioli, L.; Parenti, P.; Annoni, M. (2016) Finite element modeling of micro-orthogonal cutting process with dead metal cap, *Proceedings of the Institution of Mechanical Engineers, Part B: Journal of Engineering Manufacture*, 1-11.
- Alexandrov, S.; Mishuris, G.; Miszuris, W.; Sliwa, R. (2001) On the dead-zone formation and limit analysis in axially symmetric extrusion, *International journal of mechanical sciences*, 43(2), 367-379.
- Arrazola, P.J.; Özel, T. (2010) Investigations on the effects of friction modeling in finite element simulation of machining, *International Journal of Mechanical Sciences*, 52(1), 31-42.
- Atlati, S.; Haddag, B.; Nouari, M.; Moufki, A. (2015) Effect of the local friction and contact nature on the Built-Up Edge formation process in machining ductile metals, *Tribology International*, 90, 217-227.
- Childs, T.H.C. (2013) Ductile shear failure damage modelling and predicting built-up edge in steel machining, *Journal of Materials Processing Technology*, 213(11), 1954-1969.
- Eivani, A.; Taheri, A.K. (2008) The effect of dead metal zone formation on strain and extrusion force during equal channel angular extrusion, *Computational Materials Science*, 42(1), 14-20.
- Filice, L.; Micari, F.; Rizzuti, S.; Umbrello, D. (2007) A critical analysis on the friction modelling in orthogonal machining, *International Journal of Machine Tools and Manufacture*, 47(3), 709-714.
- Fulemova, J.; Janda, Z. (2014) Influence of the Cutting Edge Radius and the Cutting Edge Preparation on Tool Life and Cutting Forces at Inserts with Wiper Geometry, *Procedia Engineering*, 69, 565-573.
- Haddag, B.; Makich, H.; Nouari, M.; Dhers, J. (2014a) Tribological behaviour and tool wear analyses in rough turning of large-scale parts of nuclear power plants using grooved coated insert, *Tribology International*, 80, 58-70.
- Haddag, B.; Nouari, M.; Barlier, C.; Dhers, J. (2014b) Experimental and numerical analyses of the tool wear in rough turning of large dimensions components of nuclear power plants, *Wear*, 312(1), 40-50.
- Haglund, A.J.; Kishawy, H.A.; Rogers, R.J. (2008) An exploration of friction models for the chip-tool interface using an Arbitrary Lagrangian-Eulerian finite element model, *Wear*, 265(3-4), 452-460.
- Hirao, M.; Tlustý, J.; Sowerby, R.; Chandra, G. (1982) Chip Formation With Chamfered Tools, *Journal of Engineering for Industry*, 104(4), 339-342.
- Iwata, K.; Ueda, K. (1980) Fundamental analysis of the mechanism of built-up edge formation based on direct scanning electron microscope observation, *Wear*, 60(2), 329-337.
- Jacobson, S.; Wallén, P. (1988) A new classification system for dead zones in metal cutting, *International Journal of Machine Tools and Manufacture*, 28(4), 529-538.
- Jacobson, S.; Wallén, P.; Hogmark, S. (1988) Intermittent metal cutting at small cutting depths—2. Cutting forces, *International Journal of Machine Tools and Manufacture*, 28(4), 551-567.
- Johnson, G.R.; Cook, W.H. (1983) A constitutive model and data for metals subjected to large strains, high strain rates and high temperatures *Proceedings of the 7th International Symposium on Ballistic*, The Netherlands: The Hague. pp. 541-547.
- Karpat, Y.; Özel, T. (2007) Analytical and Thermal Modeling of High-Speed Machining With Chamfered Tools, *Journal of Manufacturing Science and Engineering*, 130(1), 1-15.
- Kümmel, J.; Braun, D.; Gibmeier, J.; Schneider, J.; Greiner, C.; Schulze, V.; Wanner, A. (2015) Study on micro texturing of uncoated cemented carbide cutting tools for wear improvement and built-up edge stabilisation, *Journal of Materials Processing Technology*, 215, 62-70.

- Kummel, J.; Gibmeier, J.; Schulze, V.; Wanner, A. (2014) Effect of built-up edge formation on residual stresses induced by dry cutting of normalized steel, *Advanced Materials Research*, 996, 603-608.
- Lee, D.J.; Yoon, E.Y.; Park, L.J.; Kim, H.S. (2012) The dead metal zone in high-pressure torsion, *Scripta Materialia*, 67(4), 384-387.
- Misiolek, W.; Kelly, R. (1993) Dead metal zones in extrusion of complex shapes PROCEEDINGS OF INTERNATIONAL ALUMINIUM EXTRUSION TECHNOLOGY SEMINAR: ALUMINIUM ASSOCIATION INC, & ALUMINIUM EXTRUDERS COUNCIL. pp. 315-315.
- Misiolek, W.; Kialka, J. (1996) Studies of dead metal zone formation in aluminum extrusion PROCEEDINGS OF INTERNATIONAL ALUMINIUM EXTRUSION TECHNOLOGY SEMINAR: ALUMINIUM ASSOCIATION INC, & ALUMINIUM EXTRUDERS COUNCIL. pp. 107-112.
- Movahhedy, M.R.; Altintas, Y.; Gadala, M.S. (2002) Numerical Analysis of Metal Cutting With Chamfered and Blunt Tools, *Journal of Manufacturing Science and Engineering*, 124(2), 178.
- Oliaei, S.N.B.; Karpat, Y. (2016) Investigating the influence of built-up edge on forces and surface roughness in micro scale orthogonal machining of titanium alloy Ti6Al4V, *Journal of Materials Processing Technology*, 235, 28-40.
- Özel, T. (2006) The influence of friction models on finite element simulations of machining, *International Journal of Machine Tools and Manufacture*, 46(5), 518-530.
- Qamar, S. (2010) Shape complexity, metal flow, and dead metal zone in cold extrusion, *Materials and Manufacturing Processes*, 25(12), 1454-1461.
- Segal, V. (2003a) Slip line solutions, deformation mode and loading history during equal channel angular extrusion, *Materials Science and Engineering: A*, 345(1), 36-46.
- Segal, V.M. (2003b) Slip line solutions, deformation mode and loading history during equal channel angular extrusion, *Materials Science and Engineering: A*, 345(1-2), 36-46.
- Uhlmann, E.; Henze, S.; Brömmelhoff, K. (2015) Influence of the Built-up Edge on the Stress State in the Chip Formation Zone During Orthogonal Cutting of AISI1045, *Procedia CIRP*, 31, 310-315.
- Usui, E.; Takeyama, H. (1960) I Ptiotoelastie Analysis of Machining Stresses I.
- Wallén, P.; Jacobson, S.; Hogmark, S. (1988) Intermittent metal cutting at small cutting depths—1. Dead zone phenomena and surface finish, *International Journal of Machine Tools and Manufacture*, 28(4), 515-528.
- Wan, L.; Wang, D. (2015) Numerical analysis of the formation of the dead metal zone with different tools in orthogonal cutting, *Simulation Modelling Practice and Theory*, 56, 1-15.
- Wu, J.-S.; Dillon, O.; Lu, W.-Y. (1996) Thermo-viscoplastic modeling of machining process using a mixed finite element method, *TRANSACTIONS-AMERICAN SOCIETY OF MECHANICAL ENGINEERS JOURNAL OF MANUFACTURING SCIENCE AND ENGINEERING*, 118, 470-482.
- Yamaguchi, K.; Yamada, M. (1972) Stress distribution at the interface between tool and chip in machining, *J. Engineering for Industry, Trans. ASME*, 94, 683-689.
- Zhang, H.T.; Liu, P.D.; Hu, R.S. (1991) A three-zone model and solution of shear angle in orthogonal machining, *Wear*, 143(1), 29-43.
- Zorev, N. (1963) Inter-relationship between shear processes occurring along tool face and shear plane in metal cutting, *International Research in Production Engineering*, 49, 143-152.